



Contents lists available at ScienceDirect

Biochemical and Biophysical Research Communications

journal homepage: www.elsevier.com/locate/ybbrc

IGFBP-3 and IGFBP-5 associate with the cell binding domain (CBD) of fibronectin

James Beattie ^{*,1}, Michaela Kreiner, Gordon J. Allan, David J. Flint, Diana Domingues, Christopher F. van der Walle

Strathclyde Institute of Pharmacy and Biomedical Sciences (SIBPS), University of Strathclyde, 27 Taylor St., Glasgow G4 0NR, United Kingdom

ARTICLE INFO

Article history:

Received 17 February 2009

Available online 21 February 2009

Keywords:

Fibronectin

Insulin-like growth factor binding protein

Surface plasmon resonance

ABSTRACT

We have used Surface Plasmon Resonance (SPR) – based biosensor technology to investigate the interaction of the six high affinity insulin-like growth factor binding proteins (IGFBP 1–6) with the cell binding domain (CBD) of fibronectin. Using a biotinylated derivative of the ninth and tenth Type III domains of FN (^{9–10}FNIII), we show that IGFBP-3 and -5 bind to FN-CBD. We show that this binding is inhibited by IGF-I and that, for IGFBP-5, binding occurs through the C-terminal heparin binding domain of the protein. Using site-directed mutagenesis of ^{9–10}FNIII, we show both the “synergy” and RGD sites within these FN domains are required for maximum binding of both IGFBPs. We discuss the possible biological consequences of our results.

© 2009 Elsevier Inc. All rights reserved.

Introduction

IGFBP-5 is an important regulator of the activity of both insulin-like growth factors (IGF-I and IGF-II) [1]. The affinity of IGFBP-5 for both IGFs exceeds that of cell surface IGF-I and IGF-II receptors (IGF-IR and IGF-IIR) and as such most IGFs are sequestered in binding complexes with IGFBP-5 and other high affinity IGFBPs [2]. This disparity in affinity of IGFBPs and IGFs requires the proteolysis of IGFBPs to release IGFs and allow binding to cell surface receptors [3]. IGFBP-5 and IGFBP-3 bind to other biomolecules such as components of the extracellular matrix – including heparin, osteopontin, PAI-1 and vitronectin [4–7]. Previous yeast two-hybrid studies have suggested that the interaction between IGFBP-5 and FN is mediated via the C-terminal 10th–11th Type I domains of FN [8].

In this study we have used Surface Plasmon Resonance (SPR) biosensor technology to further characterise the interaction of IGFBP-5 and IGFBP-3 with FN. In contrast to previous studies, we demonstrate conclusively that both IGFBP-3 and -5 interact with the FN cell binding domain (CBD), comprising the 9th–10th FN Type III domains (^{9–10}FNIII), which harbour the integrin $\alpha 5\beta 1$ -binding synergy (PHSRN) and RGD sites, respectively [9]. Using C-terminal mutants we show that residues within the heparin binding domain of IGFBP-5 are important for binding, although there exist subtle differences in the residues which are required for interaction with ^{9–10}FNIII compared with those required for

heparin binding. In contrast to previous studies we demonstrate that binding of IGFBP-3 and -5 to ^{9–10}FNIII is inhibited following co-incubation with IGF-I. RGD peptide had little effect on the binding of either IGFBP-3 or -5 to ^{9–10}FNIII, although mutagenesis within the PHSRN or RGD motifs of ^{9–10}FNIII inhibited IGFBP binding. We discuss the possible biological consequences of our data in relation to regulation of IGF activity in the pericellular environment.

Materials and methods

Materials. Mouse (m) IGFBP-5 expression, mutagenesis and purification has been described previously [10,11]. mIGFBP-1, mIGFBP-2, mIGFBP-3, hIGFBP-4, and mIGFBP-6 were supplied by R&D Systems (Abingdon, UK). The ^{9–10}FNIII wild type cDNA cloned into pRSET was from Prof. H. Mardon, University of Oxford. Mutation of the ^{9–10}FNIII cDNA template as directed by the amino acid substitutions described in Table 1 was made following the Quick-change™ protocol (Stratagene, Amsterdam, Netherlands). The ^{9–10}FNIII construct used in this study was a stable mutant (substituting Pro¹⁴⁰⁸ for Leu as described in [12]) extended at the C-terminus with a GGC tripeptide [13]. Using this ^{9–10}FNIII construct as a template, and showing only the sense strand, ^{9–10}FNIII-PHAAA was achieved using 5'-GAA GAT CGG GTG CCC CAC GCT GCG GCT TCC ATC ACC CTC ACC AAC C; ^{9–10}FNIII-KGD was achieved using 5'-GTG TAT GCT ACT GGC AAA GGA GAC AGC CCC GCA AGC; and ^{9–10}FNIII-GG was achieved using 5'-CCC ATT GAT TGG CCA ACA ATC AAC AGG TGG CGT TTC TGA TGT TCC GAG GGA CC (mutations underlined). The ^{9–10}FNIII proteins were biotinylated via the sulfhydryl group of the C-terminal cysteine with PEO₂-maleimide activated biotin (Pierce, UK) according to the manufacturer's

* Corresponding author.

E-mail address: J.Beattie@leeds.ac.uk (J. Beattie).

¹ Present address: Dept. of Oral Biology, Leeds Dental Institute, Clarendon Way, Leeds LS2 9LU, United Kingdom.

Table 1

Average affinity and R_{\max} values were obtained by non-linear regression of analyte concentration v Req as described in Methods section. IGFBP-3 and -5 were analysed over the concentration range 0–100 nM, in duplicate with randomised injection. The substitution levels for the $^{9-10}$ FNIII ligands are reported in the Methods section. This experiment was repeated three times and the values shown are mean \pm SD. Differences in average affinity and R_{\max} values are indicated by different letters, $p < 0.05$.

	BP-3	BP-5
<i>Average equilibrium affinities (nM)</i>		
F _n ⁹⁻¹⁰	50 \pm 13	17 \pm 3.9
F _n KGD	27 \pm 8	9 \pm 1.9
F _n PHAAA	37 \pm 4.2	10 \pm 1.8
FN GG	34 \pm 6	15 \pm 1.6
<i>R_{max}</i>		
F _n ⁹⁻¹⁰	489 \pm 32 a	825 \pm 64 a
F _n KGD	358 \pm 31 b	190 \pm 12 b
F _n PHAAA	248 \pm 13 c	131 \pm 9 c
FN GG	301 \pm 30 b	172 \pm 16 b

recommendations Biotin incorporation was estimated using the HABA (4'-hydroxyazobenzene-2-carboxylic acid) method (Pierce, UK).

Methods. Binding of IGFBP to streptavidin (SA)-immobilised biotinylated ligand using Biosensor 3000 instrumentation has been described previously [14]. For binding biotinylated $^{9-10}$ FNIII ligand, 10 μ g/ml ligand in HBS-EP buffer was applied to the surface of SA coated biosensor chips to provide substitution densities between 50 and 500 resonance units (RUs) (50–500 μ g mm^{-2}) of protein. Wt and mutant IGFBPs as analyte were present at 0–100 nM and were passed at a flow rate of 30 μ l min^{-1} across $^{9-10}$ FNIII derivatised biosensor chips. Association, dissociation and regeneration conditions were described previously [14]. The stoichiometry of IGFBP- $^{9-10}$ FNIII interaction is unknown and an average affinity for this interaction was therefore derived by non-linear regression analysis of equilibrium binding of at different analyte concentrations as described previously [14,15]. For IGF competition experiments IGFBP-3 and -5 were co-incubated with 10 μ M IGF-I overnight at 4 $^{\circ}$ C prior to analysis. The effect of mutagenesis of $^{9-10}$ FNIII was investigated by immobilisation of biotinylated $^{9-10}$ FNIII proteins at the following levels $^{9-10}$ FNIII = 603 RUs; $^{9-10}$ FNIII-KGD = 560 RUs; $^{9-10}$ FNIII-PHAAA = 610 RUs; $^{9-10}$ FNIII-GG insert = 548 RUs. Wt IGFBP-3 and -5 were present at 100 nM and were injected (5 \times) at 30 μ l min^{-1} for 5 min. Binding data are presented as the ratio IGFBP bound/ligand substitution level.

Statistics. Analysis was performed with GraphPad Prism™ using repeated measures ANOVA followed by post hoc Tukeys' *t*-test. Differences were considered significant at $p < 0.05$.

Results

Fig. 1 indicates that of the six IGFBPs only IGFBP-3 and IGFBP-5 bind to SA-immobilised biotinylated $^{9-10}$ FNIII. In these and replicate experiments, IGFBP-5 appears to bind to a greater extent than IGFBP-3 and this may be a function of the faster association rate for the former binding protein. The right hand column shows sensorgrams generated following co-incubation of IGFBPs with IGF-I and indicates that IGF-I inhibits binding of both IGFBP-3 and -5 to $^{9-10}$ FNIII is reduced.

In Fig. 2 we show the results of the binding of a panel of IGFBP-5 mutants to immobilised $^{9-10}$ FNIII and compare this with data obtained previously for binding of IGFBP-5 mutants to SA-immobilised biotinylated heparin, wherein positively charged residues within the 201–218 region of IGFBP-5 were shown to be important [11]. Here, initial studies indicated that a mutant IGFBP-5 lacking the C-terminal domain (residues 1–168) did not bind to immobi-

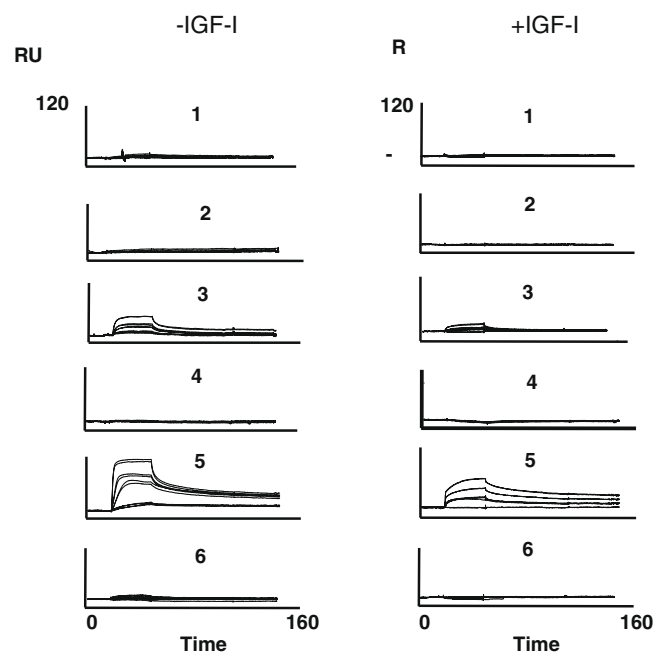


Fig. 1. IGFBP-3 and -5 bind $^{9-10}$ FNIII in an IGF-I displaceable manner. IGFBPs 1–6 were analysed at 0, 6.25, 12.5, 25, 50 and 100 nM against 88 RUs of biotinylated $^{9-10}$ FNIII. Injections were performed in a randomised order and in duplicate for each IGFBP concentration. The control flow cell contained 114 RUs BSA and the response in this cell was subtracted automatically. Responses for zero analyte have also been subtracted. Association and dissociation were for 3 and 15 min, respectively. In competition experiments IGF-I was present at 10 μ M.

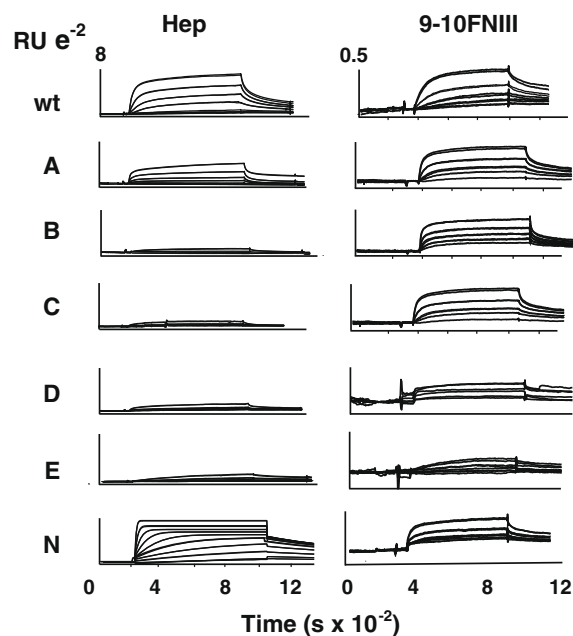


Fig. 2. Binding of IGFBP-5 mutants to heparin and $^{9-10}$ FNIII. Wt and mutant IGFBP-5 proteins (concentrations as for Fig. 1) were analysed against 524 RUs of $^{9-10}$ FNIII. Control flow cells contained 488 RUs BSA. Injection of wt and mutant proteins were randomised and duplicated. Response in control flow cells were subtracted automatically and responses for zero analyte have also been subtracted. Association and dissociation were for 8.3 and 15 min, respectively. For clarity only the first 2 min of the dissociation phase are shown.

lised $^{9-10}$ FNIII (data not shown). Although cumulative mutagenesis of positively charged residues within the C-terminal 201–218 region of IGFBP-5 result in decreased binding to $^{9-10}$ FNIII (see Fig. 2), it is clear that for $^{9-10}$ FNIII, only more highly mutated

Download English Version:

<https://daneshyari.com/en/article/10766055>

Download Persian Version:

<https://daneshyari.com/article/10766055>

[Daneshyari.com](https://daneshyari.com)